

The need for a taphonomic perspective in spatial analysis: Formation processes at the Early Pleistocene site of Pirro Nord (P13), Apricena, Italy

D. Giusti^{a,*}, M. Arzarello^b

^a*Paläoanthropologie, Senckenberg Center for Human Evolution and Paleoecology, Eberhard Karls Universität Tübingen, Rümelinstr. 23, 72070 Tübingen, Germany*

^b*Dipartimento di Studi Umanistici, Università degli Studi di Ferrara, C.so Ercole I d'Este 32, 44100 Ferrara, Italy*

Abstract

Ever since their percolation from neighbour disciplines, archaeology has employed spatial statistics to unravel, at different scales, past human behaviors from scatters of material culture. However, in the interpretation of the archaeological record, particular attention must be given to disturbance factors that operate in post-depositional processes. In this paper, we answer the need for a specific taphonomic perspective in spatial analysis by applying point pattern analysis of taphonomic alterations on the faunal and lithic assemblages from the Early Pleistocene site of Pirro Nord 13, Italy. The site, biochronologically dated between 1.3 and 1.6 Ma BP, provides evidence for an early hominin presence in Europe. The archaeological and paleontological deposits occur as filling of a karst structure that is currently exposed. We investigated the distribution of the archaeological and paleontological assemblages, as well as the distribution of identified taphonomic features, in order to evaluate the degree and reliability of the spatial association of the lithic artifacts with the faunal remains. Our results contribute to the interpretation of the diagenetic history of Pirro Nord 13 and support the stratigraphic integrity of the site.

Keywords: Spatial analysis, Point pattern analysis, Site formation processes,

*Corresponding author

Email address: domenico.giusti@uni-tuebingen.de (D. Giusti)

1. Introduction

2 Studies of site formation processes and spatial analyses have long recognized
3 the role of post-depositional factors in affecting the integrity of archaeological
4 assemblages (Hodder and Orton, 1976; Petraglia and Nash, 1987; Schick, 1984,
5 1986; Schiffer, 1972, 1983, 1987; Wood and Johnson, 1978). More recently, a
6 number of scholars have stressed the importance of establishing the degree of
7 disturbance to archaeological deposits to fully comprehend the archaeological
8 record (Dibble et al., 1997; Djindjian, 1999; Texier, 2000).

9 Besides geoarchaeological techniques, several archaeological and paleonto-
10 logical methods are widely applied to characterize the processes involved in the
11 formation of an archaeological site and to assess any post-depositional ‘back-
12 ground noise’. Taphonomy moves from its original definition (Efremov, 1940)
13 to a wider conceptual framework, targeting vertebrate assemblages, as well as
14 taphonomic entities produced by human behaviour (Domínguez-Rodrigo et al.,
15 2011). Moreover and often in joint effort, from different spatial perspectives,
16 fabric analysis (Benito-Calvo and de la Torre, 2011; Bernatchez, 2010; Bertran
17 et al., 1997; Bertran and Texier, 1995; Domínguez-Rodrigo et al., 2014c; Leno-
18 ble and Bertran, 2004; McPherron, 2005; de la Torre and Benito-Calvo, 2013);
19 refitting analysis (López-Ortega et al., 2011; Sisk and Shea, 2008; Villa, 1982);
20 vertical (Anderson and Burke, 2008) and size distribution analysis (Bertran
21 et al., 2006, 2012; Petraglia and Potts, 1994) offer meaningful contributions in
22 the unraveling of site formation and modification processes.

23 The importance of spatial statistics in the interpretation of archaeological
24 sites has long been recognized (Hodder and Orton, 1976; Whallon, 1974). How-
25 ever, studies of spatial patterning mostly focus on the behaviour of past popula-
26 tions, assuming that scatters of material culture (if not disturbed) are reflections
27 of prehistoric activities. Moreover, distribution maps still rely mainly on visual
28 examinations and subjective interpretations (Bevan et al., 2013). On the other

29 hand, quantitative methods, adopted from neighbor disciplines since the early
30 1970s (see Hodder and Orton (1976); Orton (1982); and references therein),
31 continue to promote new impulses to archaeological spatial analyses and allow
32 for the characterization of spatial patterns by adopting a more formal, induc-
33 tive approach. Recent studies (Bevan and Conolly, 2006, 2009, 2013; Bevan
34 et al., 2013; Bevan and Wilson, 2013; Crema, 2015; Crema et al., 2010; Crema
35 and Bianchi, 2013; Eve and Crema, 2014; Orton, 2004), even acknowledging
36 post-depositional effects or research biases, have continued to adopt at different
37 scales (from intra-site to regional scales) improvements in spatial statistics to
38 unravel past human behaviors from scatters of material culture. Yet, only a
39 relatively limited number of scholars have applied spatial statistics to site for-
40 mation and modification processes analysis (Carrer, 2015; Domínguez-Rodrigo
41 et al., 2014b,a).

42 In this paper, we adopt a taphonomic perspective to spatial point pattern
43 analysis of the lithic and faunal assemblages from the Early Pleistocene site of
44 Pirro Nord 13, Italy (Arzarello et al., 2007, 2009, 2012; Arzarello and Peretto,
45 2010).

46 The site (P13) provides important contributions to the ongoing debate about
47 the first hominin occurrence in Europe (Carbonell et al., 2008; Crochet et al.,
48 2009; Despriée et al., 2006, 2009, 2010; Lumley et al., 1988; Parés et al., 2006;
49 Toro-Moyano et al., 2011, 2009, 2013). A ‘Mode 1’ lithic assemblage has been
50 identified in stratigraphic association with late Villafranchian/early Biharian
51 paleontological remains. Furthermore, the presence of the Arvicoline species
52 *Allophaiomys ruffoi* correlated to the *Mymomis savini*-*Mymomis pusillus* bio-
53 zone, allows for a biochronologically refined age between 1.3 and 1.6 Ma, making
54 P13 one of the most ancient localities with human evidence currently known in
55 Western Europe (Lopez-García et al., 2015).

56 The paleontological and archaeological remains are preserved inside a com-
57 plex karst system, exposed and partially destroyed by mining activities of a
58 Mesozoic limestone quarry. The fissure P13 is a vertical fracture located at
59 the stratigraphic boundary between the Mesozoic limestone and the Pleistocene

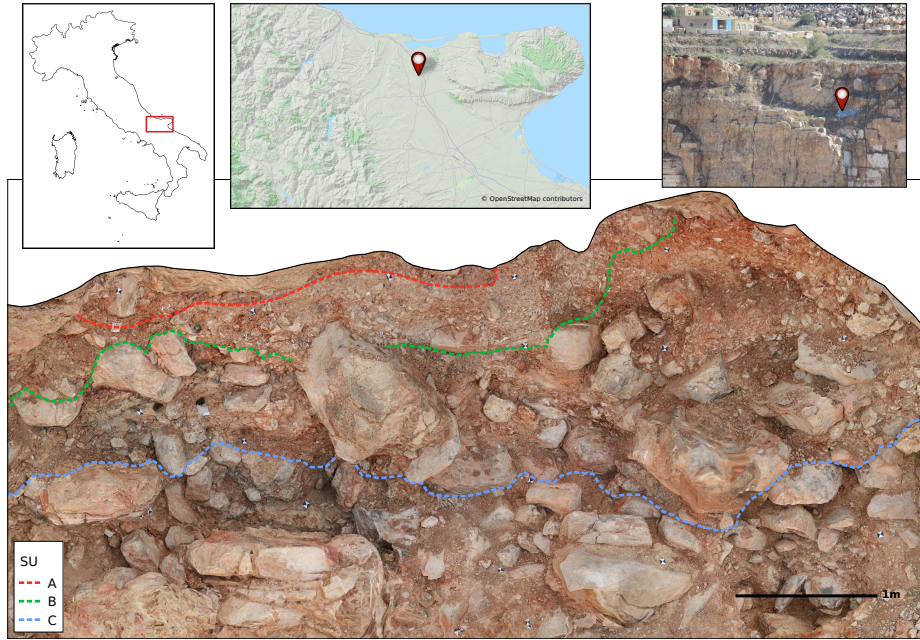


Figure 1: Geographical location of the Pirro Nord site. Picture of the fissure P13 inside the Cave Dell'Erba quarry and view of the excavated area (2013), with marked bases of the sedimentary units.

60 calcarenite formation. The deposit of the fissure is, at the time of writing, more
 61 than 4 m thick. Four Sedimentary Units (SUs) have been distinguished on
 62 lithological basis. From the top to the bottom of the section, units A to D are
 63 characterized by sediments of clayey-sand of increasing thickness (Fig. 1). Unit
 64 A includes few coarse gravels and a very low number of paleontological and ar-
 65 chaeological remains. Unit B contains more gravels, while an abrupt increase in
 66 the number and dimension of clasts and large blocks of Pleistocene calcarenite is
 67 evident within units C and D. These last units show poor size sorting of angular
 68 and sub-rounded gravels, probably correlating to a low degree of reworking that
 69 took place during a short interval of time. We also record a significant increase
 70 in the number of fossils and artifacts.

71 As a residual component of a wider karst system, it is worthwhile to assess
 72 the degree of any potential post-depositional reworking of the archaeological

⁷³ and paleontological remains and to evaluate the stratigraphic integrity of the
⁷⁴ site.

⁷⁵ The main goal of our study is to use a taphonomic perspective in spatial
⁷⁶ data analysis, in order to evaluate degree and reliability of the spatial asso-
⁷⁷ ciation of the lithic artifacts with the faunal remains that were used for the
⁷⁸ biochronological dating of the site.

⁷⁹ By applying point pattern analysis of the spatial distribution of the lithic
⁸⁰ and faunal assemblages, we aim to

⁸¹ 1. investigate the processes involved in the formation of the Pirro Nord (P13)
⁸² deposit.

⁸³ A positive spatial association of the two types of find would support the as-
⁸⁴ sumption, base on field observations, that the deposition of the archaeological
⁸⁵ and paleontological materials occurred simultaneously, as a result of subsequent
⁸⁶ mass wasting events.

⁸⁷ With the application of point pattern analysis to identified taphonomic fea-
⁸⁸ tures on the lithic and faunal assemblages, our ultimate objective is to

⁸⁹ 2. evaluate the degree of post-depositional disturbance of the site.

⁹⁰ Indeed, reworking and re-deposition processes could put in stratigraphic contact
⁹¹ materials from diverse provenience. The identification of taphonomic spatial
⁹² patterns allows us to model the spatial processes that produced them and thus
⁹³ propose a reconstruction of the agents involved in the formation and modifica-
⁹⁴ tion of the deposit.

⁹⁵ **2. Background**

⁹⁶ With the authors' permission, we integrate in our study unpublished (Bag-
⁹⁷ nus, 2011) and published (Arzarello et al., 2012, 2015) data from previous tapho-
⁹⁸ nomic studies. A brief report is presented here.

99 2.1. Taphonomy of macrovertebrate fossils

100 Taphonomic analysis (Bagnus, 2011) on macrovertebrate fossils evaluated
101 biostratinomic and diagenic processes and grouped faunal remains into different
102 sub-categories: three main taphorecords (TRs, *sensu* Fernández-López, 1987)
103 are defined according to different stages of bone surface modifications by phys-
104 ical and chemical agents (Tab. 1). Grouping was based mainly on weathering
105 (Behrensmeyer, 1978; Díez et al., 1999; Kos, 2003; Torres et al., 2003), abra-
106 sion (Behrensmeyer, 1991) and oxidation (Hill, 1982; López-González et al.,
107 2006; White, 1976; White et al., 2009), because these alterations prevail and are
108 widespread across all the sedimentary units.

109 Based on macroscopic observations of these main taphonomic features, fossils
110 from TR2 and TR3 are interpreted as re-deposited fossils: displaced bones along
111 the sedimentary surface before burial; whereas fossils from TR1 are considered
112 re-elaborated (*sensu* Fernández-López, 1991, 2007, 2011). The higher degree
113 of abrasion and the presence in the latter sub-group of multiple generations
114 of oxides, non-uniformly distributed on the fossil, are explained with repeated
115 exhumations and dislocations of previously buried elements (López-González
116 et al., 2006).

117 Therefore, a hypothetical model of site formation processes has been pro-
118 posed: animals died close to the karst sinkhole and the action of heavy rains
119 transported sediments and partially articulated carcasses into the fissure. The
120 rapid burial of fossils is confirmed by the general low degree of weathering. Karst
121 erosional processes are responsible for the very large percentage of fractured fos-
122 sils, as a result of the collapse of rock blocks from the vault. The TR1 group of
123 fossils points to internal water-flows, reworking and transportation of already
124 fossilized bones. Finally, manganese oxides that give the external widespread
125 black color to all the fossils, stones and part of the lithic artifacts are products
126 of the phreatic water fluctuation.

127 Although the taphonomic analysis definitely improved the interpretation of
128 the P13 fossiliferous deposit, the interactions between bones and karst water flow
129 have not been studied in relation to the spatial distribution and orientations of

Table 1: Contingency table of taphorecords (reproduced from Bagnus, 2011).

SU	TR1	TR2	TR3	Total by SU
A	10	30	45	85
B	26	86	114	226
C	34	69	179	282
Total by TR	70	185	338	593

¹³⁰ the skeletal elements.

¹³¹ Taking into account the inherent spatial properties of taphonomic processes,
¹³² we assume that taphogenic products (*sensu* Fernández-López, 2000) in space
¹³³ are not mutually independent and that entities which are close to each other,
¹³⁴ are likely to have followed the same genesis.

¹³⁵ Thus, in order to tackle our second objective, we analyze the spatial distribution
¹³⁶ of Fe-Mn oxides on the fossils, since the cause of their formation may derive
¹³⁷ from the action of circulating waters. Three ordinal degrees of oxidation (low,
¹³⁸ medium and high) are recognized, based on its aspect, intensity and extension.
¹³⁹ We assume that spatial aggregation of heavily-coated faunal remains (and con-
¹⁴⁰sequently segregation from non-oxidized ones) is an indication of interactions
¹⁴¹ with karst water flow.

¹⁴² *2.2. Taphonomy of lithic artifacts*

¹⁴³ The degree of natural alterations (thermal, tribological and chemical) of the
¹⁴⁴ lithic artifact surface, as a result of contact with the sediments, is a valuable
¹⁴⁵ index of integrity of the depositional context and it can usefully support spatial
¹⁴⁶ analysis in reconstructing both the past environmental conditions and the site
¹⁴⁷ formation processes (Burroni et al., 2002).

¹⁴⁸ According to a recent review of preliminary technological analyses (Arzarello
¹⁴⁹ et al., 2012, 2015), the lithic assemblage shows a general good state of preserva-
¹⁵⁰tion. If we consider the degree of patination as a good indicator of the intensity,
¹⁵¹ and not necessary of the duration, of chemical processes to which the deposit

152 has been subjected (Burroni et al., 2002), artifacts undergo non-homogeneous
153 interactions with chemical agents. Besides fresh artifacts, many of the speci-
154 mens (35%) bear Fe-Mn coatings (Fig. 2a). Iron-manganese, as well as white
155 superficial patina (5%), seems to equally affect artifacts of different flint raw
156 materials, more readily on those with a porous structure (Fig. 2b).

157 Macroscopic observations of tribological features on the assemblage reveal
158 mint to sharp, not rounded, artifact ridges and edges. Post-depositional frac-
159 tures affect 20% of the lithic material (Fig. 2c).

160 No refittings were found, as it is reasonable to expect for materials in a
161 secondary context.

162 As particle size distribution of lithic assemblages has great implications in
163 interpreting site formation processes (Bertran et al., 2012), systematic screen-
164 washing of sediments was carried out in order to guarantee recovery of lithic
165 debris, even though a very low percentage of small-size specimens has been
166 noted. This result can be initially explained either as a function of the mode of
167 knapping, which did not produce a lot of debris, or is more likely due to natu-
168 ral post-depositional processes (winnowing of low energy agents), prior to final
169 burial, possibly outside the karst fissure. Moreover, the dimensional analysis of
170 the complete lithic assemblage (Fig. 2d) does not show sorting effects.

171 We analyze the spatial distribution of taphonomic features on the lithic
172 assemblage, considering that various natural mechanisms, disturbing the spatial
173 arrangement of artifacts and sediments, will produce distinctive combinations
174 of wear features on the surfaces of lithic artifacts (Burroni et al., 2002).

175 As for the faunal assemblage, we focus the analysis on the distribution of Fe-
176 Mn patinae. Three ordinal degrees of patination (absent, spotted and covering)
177 are recognized, based on its presence and extension. In order to evaluate the
178 impact of post-depositional processes at the site, we conduct independent and
179 comparative taphonomic spatial analyses with the fossil remains.

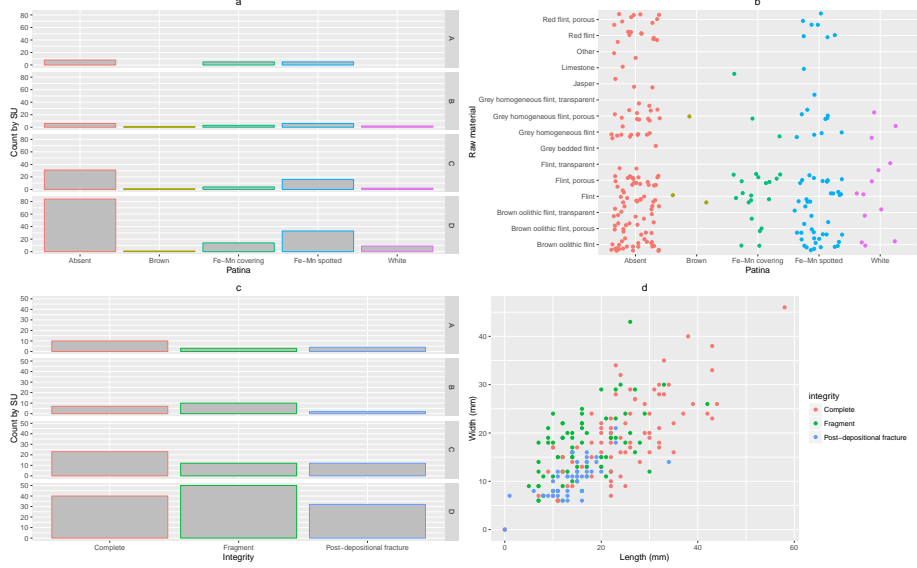


Figure 2: Frequency of patinae on the lithic assemblage, grouped by SUs (a) and their distribution on raw materials (b); frequency of fractures on the lithic assemblage, grouped by SUs (c); scatterplot of artifact dimensions (d).

180 3. Spatial data collection and sampling

181 Since 2007, systematic field investigations of the P13 fissure have been carried
 182 out by the University of Ferrara (in collaboration with the Universities of Torino
 183 and Roma Sapienza, until 2010).

184 From the first excavation season, a grid of 1 square meter units has been set.
 185 Since 2010, the three-dimensional coordinates of the finds are recorded with a
 186 Total Station, which replaced the use of a water level. Orientation (dip and
 187 strike) of coordinated faunal remains (length ≥ 2 cm), geological clasts (length
 188 ≥ 5 cm) and all the lithic artifacts is estimated with a 45 degree of accuracy,
 189 which is not precise enough for detailed fabric analysis.

190 In order to avoid possible sampling issues in spatial data analysis due to the
 191 variation in the recording methods, we select subsets of the lithic and faunal
 192 collection, excluding SUs A and B, because they have been excavated prior the
 193 use of the Total Station.

194 Focusing on SUs C and D, we scale the windows of analysis according to
195 the extension of excavated areas for each SU, excluding the presence of the
196 large blocks of rock. We reduce in this way the impact of the Modifiable Area
197 Unit Problem (MAUP) in point pattern analysis (Openshaw, 1996), especially
198 insidious in this study due to the particular geological setting of the site. The
199 analyzed areas of SUs C and D are respectively 4.34 m^2 and 5.82 m^2 .

200 During 6 years of excavations, more than 1600 of 2152 macrovertebrate fossils
201 have been spatially recorded: 471 from SU C and 916 from SU D. However,
202 Bagnus (2011) conducted taphonomical analysis on fossils recovered during the
203 2007 to 2010 field seasons and only 593 of these are classified in one of the
204 three taphorecords (Tab. 1). Our sample includes 135 coordinated elements
205 of the 282 analyzed fossils from SU C. From the total number of 366 lithic
206 artifacts collected until the 2014 field season, 147 have been recorded with three-
207 dimensional coordinates. Our sample includes 34 lithics from SU C and 84 from
208 SU D. From the micro-mammal assemblage, we include in this study only the
209 *Allophaiomys ruffoi* species. Of the 53 arvicoline teeth collected from the screen-
210 washed sediments, 49 have secure provenance attribution from SU B ($n = 2$),
211 C ($n = 14$) and D ($n = 33$) (Lopez-García et al., 2015). However, the *A. ruffoi*
212 point pattern does not represent the exact distribution of the remains. Indeed,
213 we randomly displaced ($r = 0.5$) each point indicating the provenience of the
214 sieved sediment.

215 **4. Vertical distribution**

216 The vertical distribution of finds is a key factor in the analysis of site forma-
217 tion processes. Many processes can be well approximated by a ‘nearly’ normal
218 distribution. However, testing the appropriateness of this assumption is an es-
219 sential step in spatial data analysis. Strongly right skewed distribution would
220 occur in case of a non-uniform vertical distribution of finds; thus requiring the
221 analysis to acknowledge the covariate effect of gravity in the observed spatial
222 pattern.

223 The vertical distribution of finds within SU C is globally unimodal, roughly
224 symmetric (slightly left skewed), in spite of some outliers (Fig. 3a). It ‘nearly’
225 approximates the maximum-likelihood fitting of a normal curve (red line) with
226 mean (μ) = −1.53 m and standard deviation (σ) = 0.27 m. However the Shapiro-
227 Wilk normality test rejects the null hypothesis of a gaussian distribution ($p -$
228 value = 0.0005). On the other hand, the Q-Q plot (Fig. 3b) shows deviations
229 from the theoretical normal distribution (red line) between one (68.27% of the
230 sample) and two (95.45%) standard deviations from the mean. The S-shaped
231 empirical distribution recalls its left skew.

232 The global vertical distribution of finds resemble that of the faunal assem-
233 blage, due to the weight of the latter on the sample data ($n = 471$). The
234 distribution of the lithic artifacts is more left skewed, while the small sample
235 of micromammals follows a multimodal distribution with a prominent peak at
236 −1.2 m (Fig. 3a). Although the difference in size of the two samples, it is worth
237 notice that the mean value of the vertical distribution of *A. ruffoi* is very close
238 to that of the lithic artifacts (Welch Two Sample t-test $p - value = 0.5803$).

239 The vertical distribution of finds in SU D is globally unimodal, slightly left
240 skewed, with one peak at −2.10 m and no outliers (Fig. 3c). Although the dis-
241 tribution is close to the best fitting normal curve (red line) with $\mu = -2.34$ m
242 and $\sigma = 0.33$ m, the Shapiro-Wilk test rejects the hypothesis of normality
243 ($p - value = 2.497e - 12$). The Q-Q plot (Fig. 3d) shows a more dispersed dis-
244 tribution with respect to the former one. Its steeper line follows the theoretical
245 normal distribution within one standard deviation from the mean (68.27% of
246 the sample).

247 Compared with the global distribution, the vertical distribution of lithic
248 artifacts slightly skews to the right. Nevertheless, the Shapiro-Wilk test fails
249 to reject the normality hypothesis ($p - value = 0.2742$). On the other hand,
250 the micromammal distribution is multimodal and slightly shifted to the right
251 (Fig. 3c). Its mean (−2.284 m) is quite close to the mean of the lithic sample
252 (−2.423 m). However, the Welch t-test rejects the hypothesis of two equal
253 sample means ($p - value = 0.0141$). If we cannot state that the two distributions

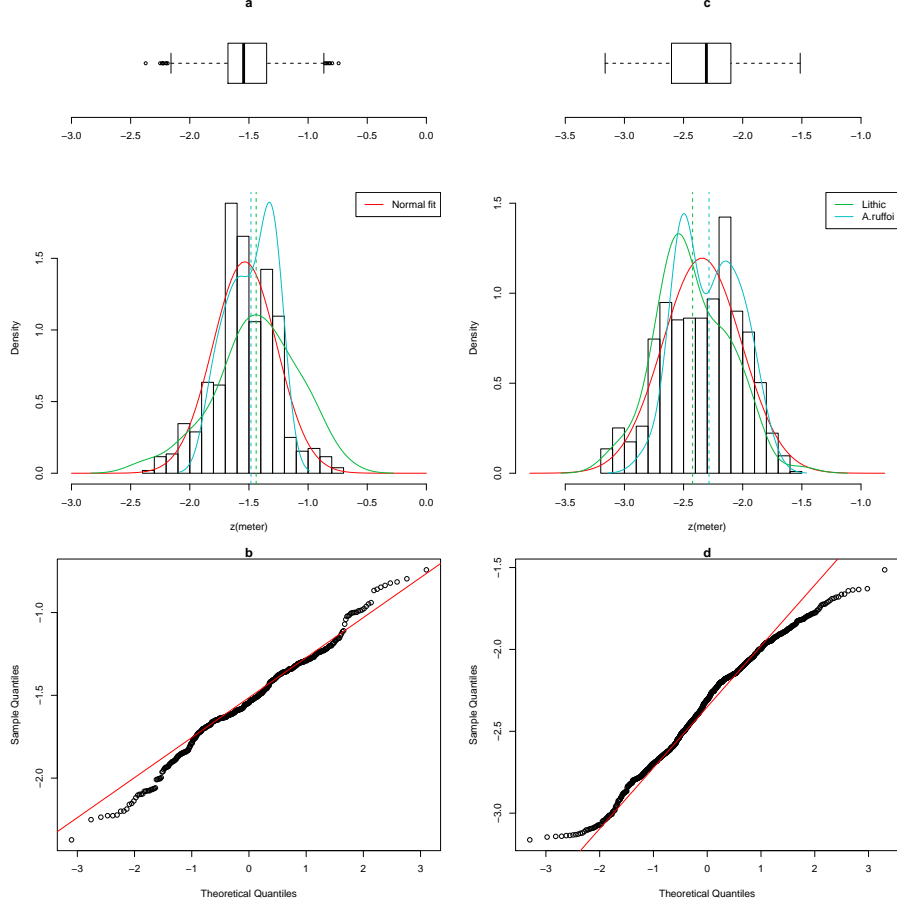


Figure 3: Vertical distribution of finds in SU C (a,b) and D (c,d).

254 have the same mean, we remark the highest density of both the assemblages at
 255 around -2.5 m.

256 As for the vertical distribution of the identified taphonomic features on the
 257 lithic and faunal assemblages, Fig. 4a,b illustrates the overall distribution of
 258 patinae on the lithic artifacts, across SU C and D. The histogram shows the
 259 increasing number of finds between the two sedimentary units. This trend is
 260 reflected as well in the rise of Fe-Mn patinated artifacts (41% in SU C and 45% in
 261 SU D), compared to non-patinated ones (respectively 50% and 48%). The kernel
 262 density estimation (blue and green lines) shows a slightly higher occurrence of

²⁶³ patinated artifacts at the lower part of the sequence (below -2.5 m), whereas in
²⁶⁴ SU C (up to -2 m) there is no evident preference in the vertical distribution of
²⁶⁵ patinae. The higher density of patinated artifacts, linked to the concentration
²⁶⁶ of lithics observed in Fig. 3c at about -2.5 m, can be localized in a restricted
²⁶⁷ spot at the bottom right corner of the excavated area (Fig. 4a).

²⁶⁸ Restricting the analysis to SU C, the vertical distribution of coordinated
²⁶⁹ macrovertebrate fossils analyzed by Bagnus (2011) spans 71% of the elevation
²⁷⁰ range of the complete assemblage from the same SU. However, being only the
²⁷¹ 29% of the population, we acknowledge that our sample cannot be considered
²⁷² representative.

²⁷³ The densities of the low and medium rate of oxides resemble the general dis-
²⁷⁴ tribution (Fig. 4c,b). Low values follow a ‘nearly’ normal distribution (Shapiro-
²⁷⁵ Wilk normality test $p-value = 0.2186$). The density of high oxidized remains
²⁷⁶ (54% of the sample) draws a left skewed distribution, with a peak at about
²⁷⁷ -1.3 m; whereas fossils with a medium degree of oxides are skewed to the right.
²⁷⁸ However there is no clear preference for oxides to occur deeper in the sequence.
²⁷⁹ The mean values are very close to each other and lower values of oxides are
²⁸⁰ more dense at the bottom of the SU.

²⁸¹ As for the distribution of the three taphorecords, the prominent peak of TR1
²⁸² at -1.6 m (Fig. 4f) contrasts with a more distributed and mixed distribution of
²⁸³ the second and third groups of fossils. However, the very low frequency of TR1
²⁸⁴ ($n = 9$) limits further analyses.

²⁸⁵ Although our study is constrained by the small sample of fossils and by its
²⁸⁶ limited spatial extension to SU C, the analysis of the vertical distribution of Fe-
²⁸⁷ Mn oxides in the faunal and lithic assemblages does not show any clear global
²⁸⁸ pattern. Indeed, even taking into account the localized cluster of artifacts at the
²⁸⁹ very bottom of SU D (Fig. 4a), the process responsible for the distribution of
²⁹⁰ Fe-Mn oxides seems to operate indistinctly through the complete stratigraphic
²⁹¹ sequence, with no explicit preference for lower elevations.

²⁹² With no evidence for strong right skewed distributions of finds in SUs C
²⁹³ and D, we have reasons to exclude the covariate effect of gravity in the observed

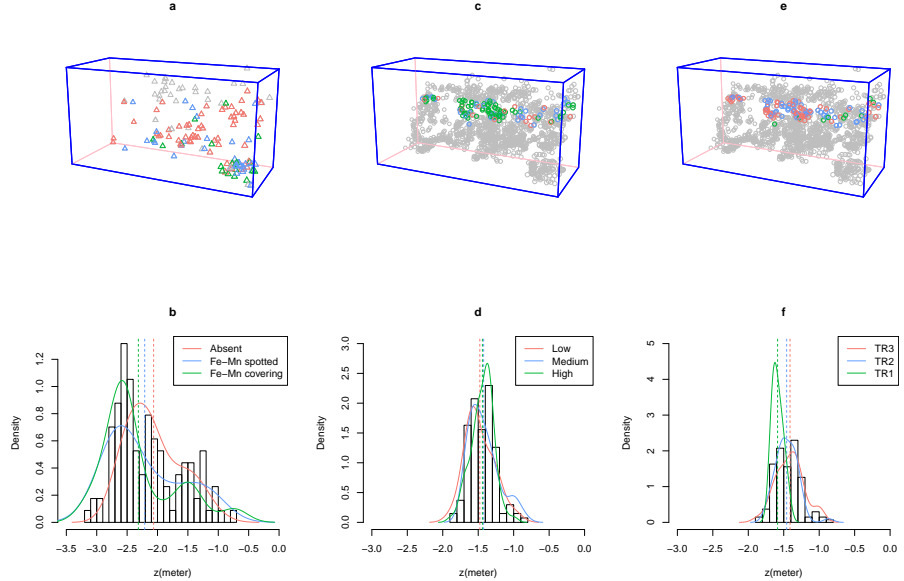


Figure 4: 3D and vertical distributions of Fe-Mn patinae on the lithic assemblage from SUs C and D (a,b); oxides (c,d) and taphorecords (e,f) from the faunal sample.

294 spatial pattern. The subsequent point pattern analyses are directed to the study
 295 of the 2D spatial distribution of fossils, lithics and their taphonomic status.

296 5. Point pattern analysis

297 The observed patterns of the archaeological and paleontological remains
 298 within SUs C and D, as well as the patterns of taphonomic features recog-
 299 nized on them, have been treated as realizations of spatial point processes, i.e.
 300 site formation and modification processes.

301 Indeed, a spatial point pattern is generally defined as the location of events
 302 generated by a point process, operating simultaneously at different scales: a
 303 first-order global scale and a second-order local scale (Bailey and Gatrell, 1995).
 304 The former results from the frequency (density) of events within a bounded
 305 region; the latter results from spatial dependency between points, e.g. from
 306 a tendency for values of the process at nearby locations to interact with each

307 other. Three different types of interpoint interaction are possible: random (or
308 Poisson); regular and cluster. Regular patterns are assumed to be the result of
309 inhibition processes, while cluster patterns are the result of attraction processes.
310 Therefore, two main issues of interest are explored by spatial point pattern
311 analyses: the distribution (density) of entities in space and the existence of
312 possible interactions between them (Ord, 1972).

313 First-order effect in the observed point-pattern is generally non-parametrically
314 evaluated by means of kernel density estimation (Diggle, 1985). As an average
315 density of points in the study region, intensity informs about uniform or inho-
316 mogeneous distribution of events.

317 Multiple scales of second-order patterning and the probability of a stochastic
318 occurrence are explored by the Ripley's K summary function (Ripley, 1976,
319 1977) and derivates, for both univariate and bivariate point patterns. The K
320 function is designed to identify the relative aggregation and segregation of point
321 data at different scales. The univariate $K(r)$ function measures the expected
322 number of events found up to a given distance r around an arbitrary event.
323 By comparing the estimated value $\hat{K}(r)$ to its theoretical Complete Spatial
324 Randomness (CSR) value, it is possible to assess what kind of interaction exists
325 between events. The bivariate function, or cross-type $K_{ij}(r)$ function seeks to
326 evaluate, at each distance r , the spatial relation between two types ij of observed
327 events. In this case, the definition of the null hypothesis uses a randomization
328 technique of either the location of one of the types (random shift hypothesis),
329 or the type itself of the event at each point, preserving the original location
330 (random labeling hypothesis) (Goreaud and Péllissier, 2003). The former aims to
331 evaluate the spatial relationship between patterns of two independent processes,
332 while the latter assumes the same process in determining the pattern for different
333 types.

334 Especially in small dataset, the estimation of correlations between points is
335 biased by edge effects, arising from the unobservability of points outside the
336 window of analysis. In order to reduce that bias, we implement here Ripley's
337 isotropic edge correction (Ripley, 1988; Ohser, 1983).

Monte Carlo simulations (Robert and Casella, 2004) are used to generate pointwise critical envelopes of random expected values for the null hypotheses, providing an adequate level of statistical significance. We choose a small significance level ($\alpha = 0.01$ obtained with 199 simulations), due to the higher possibility of committing a Type 1 error by testing our hypotheses. Values of the empirical distribution (black solid line) are plotted against the theoretical Poisson distribution (red dotted line) and the simulated global envelope of significance (grey area). For $K(r)$, when the solid line of the observed distribution is above or below the shaded grey area, the pattern is significantly clustered (points are closer together than would be expected for a complete random pattern) or dispersed. For $K_{ij}(r)$, the benchmark value πr^2 is consistent with independence between the points of types i and j , and does not imply a Poisson distribution.

5.1. Formation processes

In order to investigate the processes involved in the formation of the Pirro Nord deposit, we provisionally assume the deposition of each sedimentary unit to be the result of mass wasting events filling the fissure and resulting in the distribution of fossils and artifacts independently of each other.

To test the appropriateness of our working assumption, we first analyze the overall distributions of finds, treated as univariate point patterns. Applying a set of exploratory statistics, we aim to determine the nature of the depositional processes, e.g. if they raise in- or homogeneous distributions. Then, we analyze the relative patterns of the faunal and lithic assemblages from SUs C and D. In this case, we treat the two distributions as multitype point patterns.

The intensity of the lithic and faunal assemblages is non-parametrically estimated by first performing a Gaussian smoothing kernel of their distributions, for both SUs. Likelihood cross-validation bandwidth, which assumes an inhomogeneous process, is selected for each pattern. Edge correction is applied using the method of Diggle (1985). Then, Berman's Z_2 test is used to determine whether or not the intensity depends on a spatial covariate Z , assuming that the spatially

368 varying (inhomogeneous) intensity is a function of Z . Thus, in order to measure
369 the strength of dependence on the covariate, we use the Receiver Operating
370 Characteristic (ROC) curve. Spatially adaptive smoothing, nearest-neighbour
371 density and scan tests have been used in order to assess for the evidence of
372 hot spots in the intensities of the unmarked point patterns. Estimations of
373 the $K(r)$ and the Kaplan-Meier corrected empty-space $F(r)$ functions provide
374 further methods for the interpretation of the distributions.

375 Multitype summary functions are used in the analysis of the dependence
376 between points of the two assemblages. In this case, our main research question
377 is whether different types of finds have the same spatial distribution. The cross-
378 type $K_{ij}(r)$ function and the Kaplan-Meier corrected nearest-neighbour $G_{ij}(r)$
379 function are used to estimate the association between points of types i and
380 j , for any pair of types of finds. Positive spatial correlation between the two
381 types of finds would suggest that lithic artifacts are more likely to be found
382 close to fossils than would be expected for the hypothesis of *independence*. It
383 would confirm the field observations about their close stratigraphic association
384 and further support our hypothesis that both patterns are the realization of
385 one depositional process. On the other hand, segregation of the two patterns
386 is equivalent to variation in the probability distribution of types. Segregation
387 could be interpreted as the expression of preferential/differential depositional
388 processes. In this case, more detailed analyses would be necessary.

389 *5.2. Post-depositional processes*

390 In order to evaluate the degree of post-depositional disturbance of the de-
391 posit, the spatial dependence of observed taphonomic features is assumed to
392 be the expression of a related diagenetic process. Measured phenomena that
393 are closer together in space, tend to be more related than those further apart
394 (Tobler, 1970).

395 Like in applications of point pattern analysis in spatial epidemiology (Diggle,
396 2003; Gatrell et al., 1996), we distinguish between *cases* and *controls*. The
397 distribution of cases of a certain taphonomic alteration can be regarded as the

398 realization of a diagenetic point process, whereas control points refer to non-
399 altered remains. In a conditional analysis of a spatial case-control study the
400 locations are fixed covariates, and the taphonomic status is treated as a random
401 variable. The simplest null model (*random labelling*) is that the taphonomic
402 status of each find is random, independent and with constant risk of occurrence.

403 Spatial correlations of diagenetic alterations on the lithic and faunal assem-
404 blage are explored by the $K_{ij}(r)$ function, random labelling the pair case/control
405 of Fe-Mn oxidation. We assume in this case that an independent process (karst
406 water circulation), subsequent to the initial event responsible for the accumu-
407 lation of the finds in each SU, determined their preservation status. Positive
408 deviations from the null hypothesis, suggest that cases are more likely to be
409 found close to controls than would be expected if their status was randomly
410 determined. On the other hand, negative deviations would indicate segregation
411 between cases and controls. Thus, it would suggest that the action of post-
412 depositional water-related processes could have locally reworked the original
413 distribution, determining the altered status of the remains.

414 All the spatial analyses were performed using the *spatstat* package (Baddeley
415 et al., 2015) in R statistical software (R Core Team, 2015).

416 A repository containing a compendium of data, source code and text is
417 archived at the DOI: 10.5281/zenodo.54778.

418 **6. Results**

419 *6.1. Formation processes*

420 Fig. 5c,d shows the smoothing kernel estimation of the faunal assemblage
421 intensity respectively in SUs C and D. Lithic artifacts and micromammals re-
422 mains of *A. ruffoi* are superimposed on it. The visual assessment of the plot
423 suggests positive spatial association between the three types of finds. Higher
424 intensities in the distributions are evident at specific values of the x coordinate
425 ($6 < x < 7$ and $8 < x < 9$), in both the sedimentary units. Yet, a concentration
426 of artifacts, already observed in Fig. 3c and 4a,b, is evident at the lower right

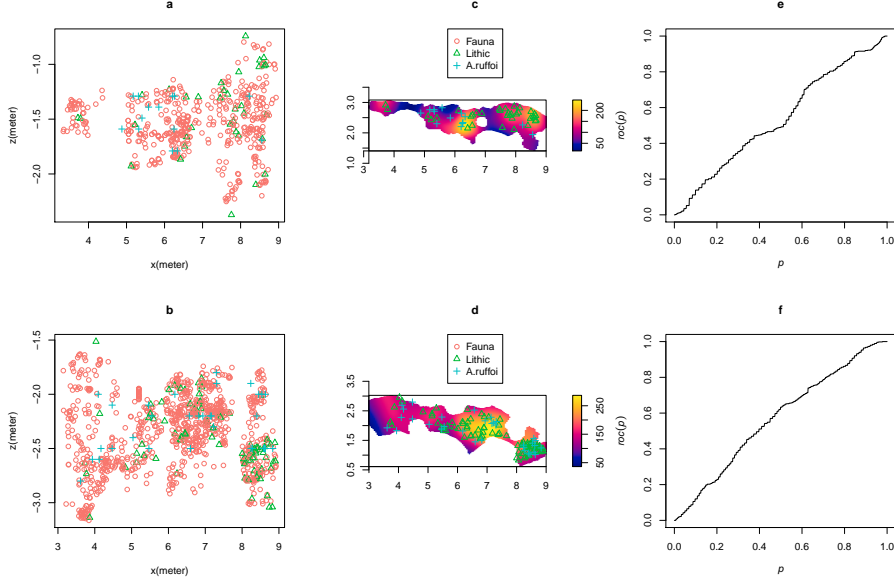


Figure 5: Scatterplot of finds from SU's C (a) and D (b); Smooth density estimation of the faunal assemblage and distribution of lithic artifacts and *A.ruffoi* remains in SU's C (c) and D (d); ROC curves for the covariate x coordinate in SU's C (e) and D (f).

corner of SU D (Fig. 5e). Such higher densities of finds are clearly shown as well in the scatterplots of the projected third coordinate (Fig. 5a,b). Notably, the thickness of the sedimentary unit cannot be accounted to be responsible for those hot spots with higher density of finds. Neither the apparent inhomogeneous intensities along the x axes are supported by the ROC curves (Fig. 5e,f). Even if Bermans's Z_2 tests suggest significant evidence of dependence on the x covariate, the ROC curves show that it does not have strong discriminatory power.

Fig. 6a,d shows the resulting p -values of likelihood ratio scan test statistic. The test detects differences in the densities of the distributions, showing zones with high abundance of finds. The estimated homogeneous $\hat{K}(r)$ and $\hat{F}(r)$ functions are consistent with this result. For both SUs C (Fig. 6b,c) and D (Fig. 6e,f) they suggest strong deviation from the null hypothesis of CSR towards aggregation, at any scale.

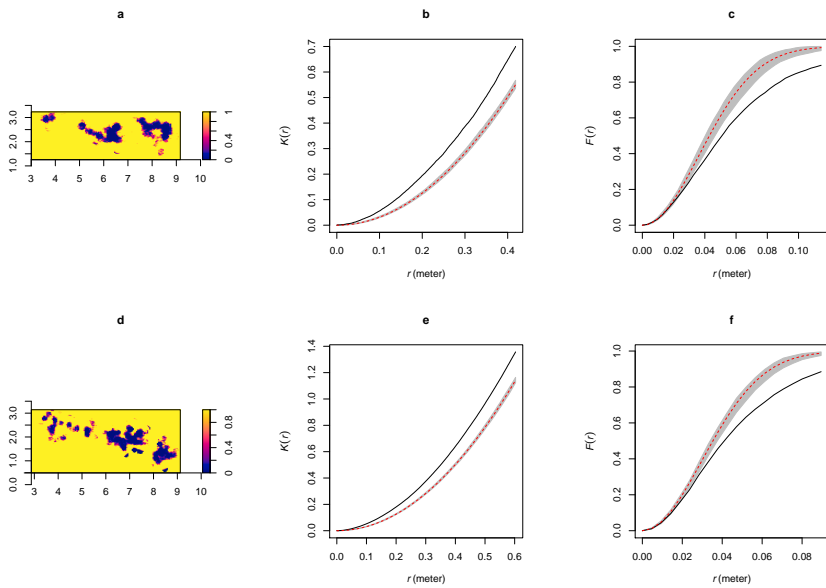


Figure 6: p-values of the likelihood ratio scan test, with logarithmic colour scale, for SUs C (a) and D (d); pointwise envelopes of the homogeneous $K(r)$ and $F(r)$ functions for unmarked finds from SUs C (b,c) and D (e,f).

441 In analyzing a point pattern, it is confounding and it may be impossible
442 to distinguish between clustering and spatial inhomogeneity (Baddeley et al.,
443 2015). Given the context of the site, and the results of our non-parametric
444 analyses, we proceed considering the distributions of finds as the results of clus-
445 ter homogeneous processes. The bivariate version of the homogeneous $K_{ij}(r)$
446 and $G_{ij}(r)$ functions allows us to statistically test the hypothesis of aggregation
447 between the types of remains.

448 In Fig. 7, the top line of panels (a,b,c) shows the ordinary estimations of the
449 K function for the three types of finds (Fauna, Lithic and *A. ruffoi*) from SU
450 C. Panel 7a resembles figure 6b and indicates statistical significant clustering of
451 the faunal remains for any values of r . The lithic assemblage shows as well a
452 significant cluster tendency, for $r > 0.1$, while it fails to reject the null hypothesis
453 of CSR for lower values. Instead, the estimated $\hat{K}(r)$ for the micromammals
454 shows aggregation, but, for all values of r , we cannot state that the distribution
455 is not random. This result might reflect the random displacement applied to
456 the micromammal point pattern.

457 The middle and bottom lines of panels in Fig. 7 show estimations of the
458 homogeneous cross-type K and G functions for all pairs of types i and j . Inter-
459 estingly, Fig. 7d suggests positive spatial correlation between lithic and faunal
460 remains at any values of $r > 0.05$. The corresponding $G_{ij}(r)$ function mea-
461 sured the cumulative distance from each point of type i (Lithic) to the nearest
462 point of type j (Fauna). It shows (Fig. 7g) that the nearest-neighbour distances
463 are significantly shorter than expected, but we cannot reject the hypothesis of
464 independence between fossils and artifacts. However, the short scale of the func-
465 tion suggests that any artifact is surrounded by fossils. This result statistically
466 confirms the stratigraphic association of artifacts and fossils, previously based
467 on field observations. On the other hand, deviations between the $\hat{K}_{ij}(r)$ func-
468 tion and the benchmark πr^2 suggest segregation between lithics and *A. ruffoi*
469 specimens, but the hypothesis of independence between the two types is more
470 significant (Fig. 7e,h). Conversely, the small mammal assemblage is closer to
471 the rest of the fossils than expected for independent distributions, for $r > 0.2$.

⁴⁷² For lower values of r , the K and G functions fail to reject the hypothesis of
⁴⁷³ independence.

⁴⁷⁴ The top line of panels in Fig. 8 (a,b,c) shows estimations of the $K(r)$ function
⁴⁷⁵ for the three types of finds from SU D. Panel 8a confirms the same clustering
⁴⁷⁶ trend of the faunal assemblage. Analogous to the distribution of finds from SU
⁴⁷⁷ C, the global pattern is mostly weighted on the faunal assemblage (Fig. 6e).
⁴⁷⁸ Conversely, in SU D the distribution of lithics shows stronger significant clus-
⁴⁷⁹ tering for $r > 0.1$. Again, the resulting $\hat{K}(r)$ for the micromammal assemblage
⁴⁸⁰ suggests a statistically insignificant aggregation tendency for all values of r , but
⁴⁸¹ $0.4 < r < 0.5$. In contrast to the previous result, estimations of the $K_{ij}(r)$
⁴⁸² function support significant positive correlation between the lithic artifacts and
⁴⁸³ the *A. ruffoi* remains (Fig. 8e). Thus, they occur closer than expected in the
⁴⁸⁴ case of independent distributions. Panel 8f shows the same positive correlation
⁴⁸⁵ also between micro- and macro-mammals for $r > 0.2$. The panels 8d,g show
⁴⁸⁶ as well a significant positive aggregation between lithics and fossils for values
⁴⁸⁷ of $r > 0.1$. In addition, the estimated $\hat{G}_{ij}(r)$ function offers a closer view
⁴⁸⁸ of the distribution. For values of $r < 0.1$, it fails to reject the hypothesis of
⁴⁸⁹ independence.

⁴⁹⁰ *6.2. Post-depositional processes*

⁴⁹¹ To achieve our second objective, namely to evaluate the degree of post-
⁴⁹² depositional disturbance of the deposit, we first analyzed spatial distribution of
⁴⁹³ oxides on the lithic and faunal assemblages independently, then we moved to a
⁴⁹⁴ comparative analysis. We are particularly interested in the spatial distribution
⁴⁹⁵ of Fe-Mn oxides (cases) compared with the absence of them (controls).

⁴⁹⁶ Fig. 4a does not suggest segregation of patinated and not-patinated lithics.
⁴⁹⁷ If we perform random labeling of the presence of Fe-Mn (spotted and covering)
⁴⁹⁸ with its absence in both the stratigraphic units, the outputs of the cross-type
⁴⁹⁹ function (Fig. 9a, b) show that the observed altered artifacts are, with a 0.01
⁵⁰⁰ level of significance, randomly and independently located in SU C. The positive
⁵⁰¹ discrepancy between the estimated $\hat{K}_{ij}(r)$ and the benchmark πr^2 indicates

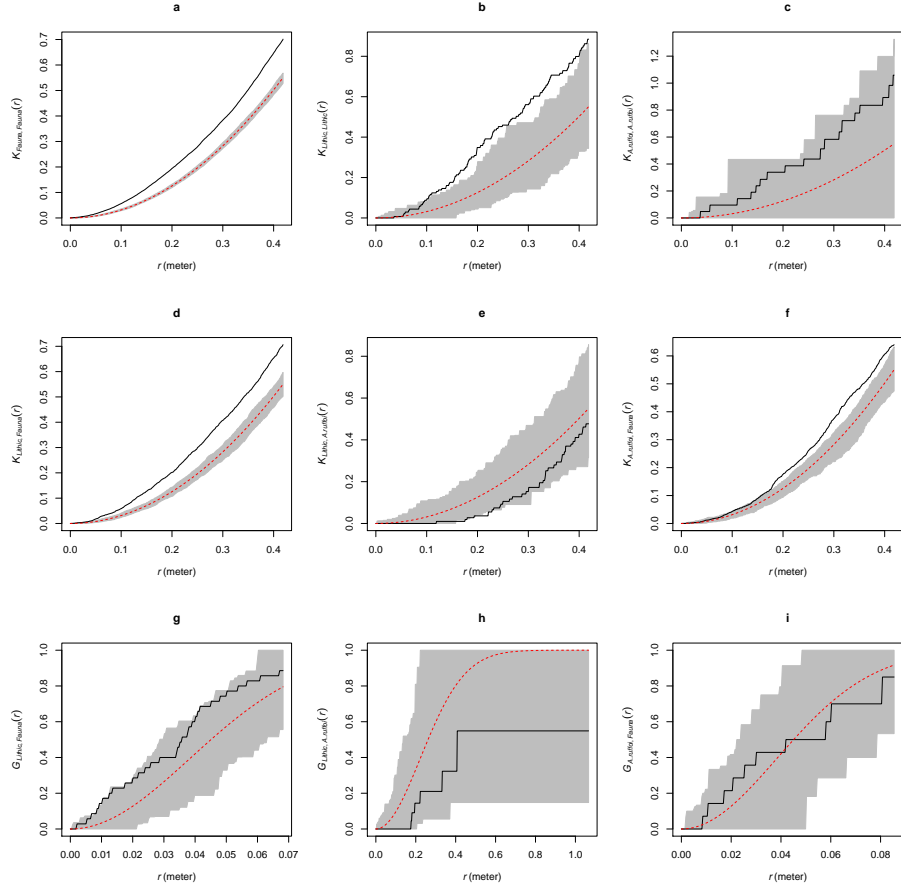


Figure 7: Pointwise envelopes of the homogeneous cross-type $K_{ij}(r)$ and $G_{ij}(r)$ functions for all pairs of types i and j in SU C.

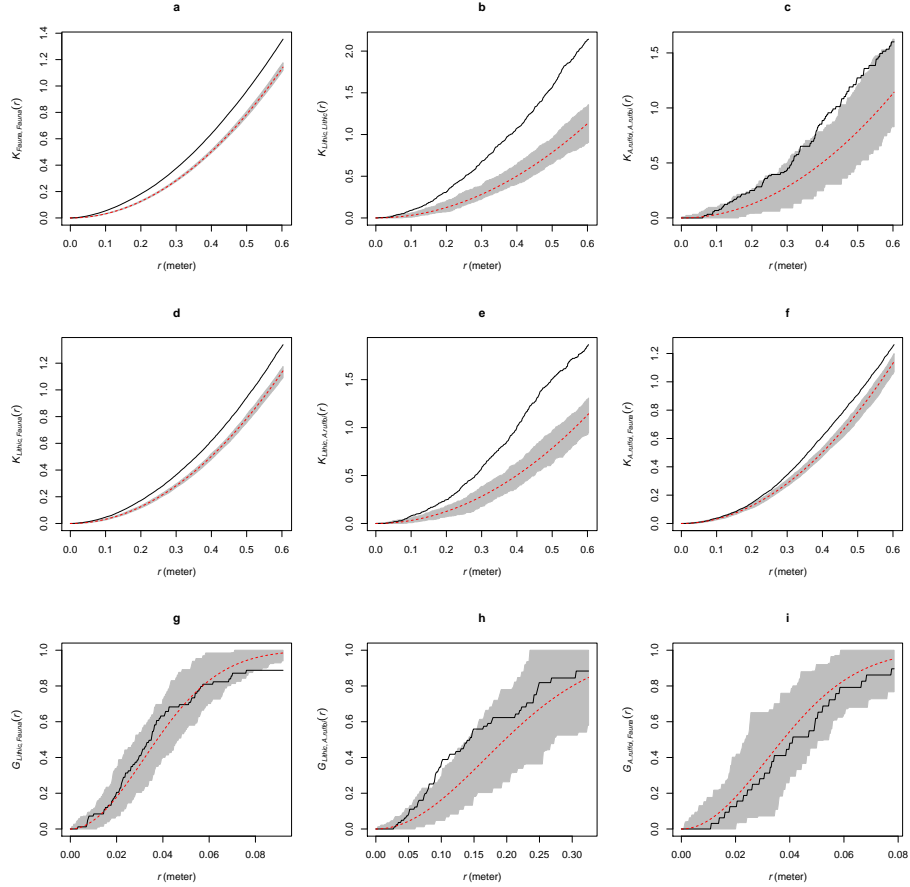


Figure 8: Pointwise envelopes of the homogeneous cross-type $K_{ij}(r)$ and $G_{ij}(r)$ functions for all pairs of types i and j in SU D.

502 aggregation of cases and controls, but it lies within the grey envelope of the
503 *random labeling* hypothesis. Conversely, patinated and non-patinated lithics in
504 SU D appear to be closer to each other than expected for the null hypothesis.
505 In this unit the observed $\hat{K}_{ij}(r)$ function over-exceeds the envelope at values of
506 $r > 0.4m$, hence it indicates statistically significant aggregation. Such pattern
507 statistically confirms the visual assessment of figure 4a. Consequently, oxidized
508 and non-oxidized artifacts most probably occur in SU D well aggregated in
509 space, while their aggregation is not statistically significant in the above unit.

510 We could not compare the oxidation patterns between lithics and fossils from
511 SU D, because the taphonomic analysis of Bagnus (2011) did not include fossils
512 from this unit. Thus, we focused our analysis on SU C.

513 The distribution map (Fig. 4c) does not suggest any evident pattern. When
514 we apply random labelling of the absence of oxidation with the medium and high
515 degrees of its presence, the output of the bivariate $K_{ij}(r)$ function shows a seg-
516 regation tendency between them, but it is not statistically significant. (Fig. 9c).
517 A random and independent distribution of oxides is more plausible.

518 Finally, Fig. 9d shows the result of the $K_{ij}(r)$ function, random labeling
519 the cases (medium and high degrees) and controls (absent or low degree) of
520 Fe-Mn oxides on the lithic and faunal assemblages from SU C. The empirical
521 values of the cross-type function are balanced on the theoretical expectation
522 for complete spatial independence (red line). It clearly lies inside the grey
523 envelope of significance. Therefore, our analysis shows an independent spatial
524 distribution of Fe-Mn patinated and non-patinated lithic artifacts and fossils
525 from SU C. In the lower unit (SU D), where Fig. 4b indicates higher density of
526 oxidized artifacts, estimations of the cross-type K function suggests that they
527 occur closer than expected to fresh ones.

528 **7. Discussion**

529 The Early Pleistocene site of Pirro Nord (fissure P13) has yielded evidence
530 for one of the earliest occurrences of hominins in Europe. The importance of the

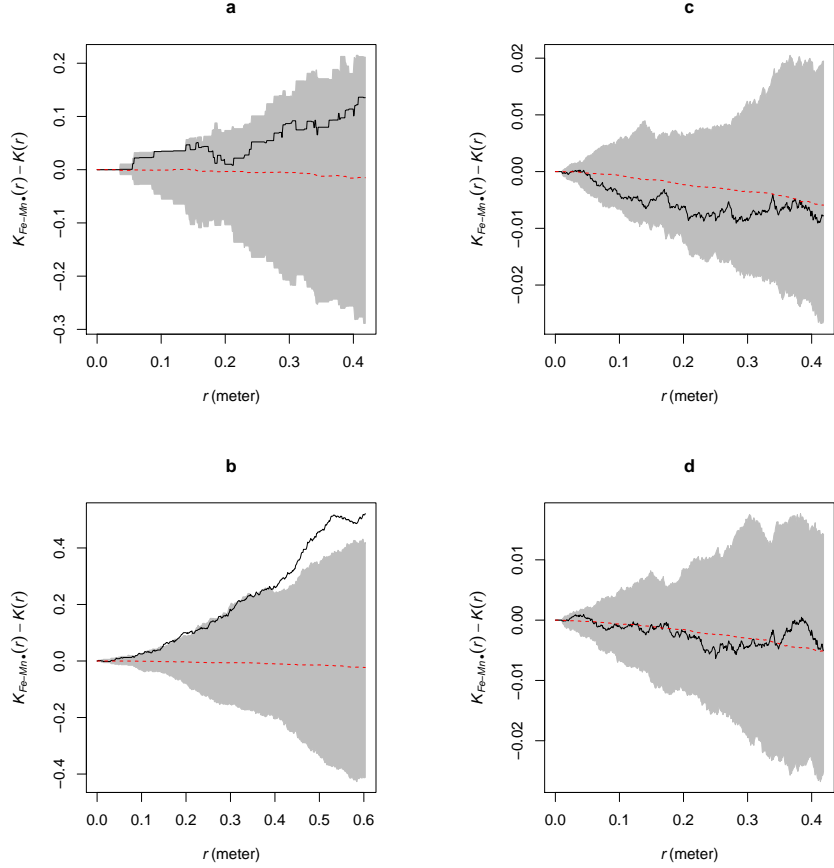


Figure 9: Pointwise envelopes of the homogeneous bivariate $K_{ij}(r)$ function, random labeling cases/controls of patinated lithics in SUs C (a) and D (b); oxidated fossils in SU C (c); Fe-Mn oxides on the lithic and faunal assemblages from SU C (d).

531 evidence calls for a multivariate taphonomic analysis in order to establish the
532 nature of the processes involved in the formation of the deposit and the degree
533 of its post-depositional disturbance. We address that need by investigating the
534 spatial association of the archaeological and paleontological remains, as well as
535 the spatial distribution of artifacts and fossils with diagenetic alterations. We
536 focused our analysis on the lower stratigraphic units C and D, since they provide
537 the most significant corpus of finds and they have been studied with the same
538 research protocol.

539 *7.1. Formation processes*

540 Non-parametric analyses have been carried out in order to characterize the
541 processes responsible for the formation of the deposit. Then, we accounted for
542 the relative spatial pattern of the different types of finds.

543 The vertical distribution of the archaeological and paleontological assem-
544 blages does not appear to be affected by strong gravitational effects. On the
545 other hand, it resembles a 'nearly' normal distribution and suggests a very close
546 mean occurrence of lithic artifacts and *A. ruffoi* remains, despite the small sam-
547 ple of micromammals (Fig. 3). A visual interpretation of the projected third
548 coordinate (Fig. 5a,b) also suggests that the intensity of finds is not a function
549 of the covariate z . Moreover, higher densities are not linked to the thickness of
550 the stratigraphic units. They are clearly localized at values of $6 < x < 7$ and
551 $8 < x < 9$ in both the SUs, as shown also by Fig. 5c,d and 6a,d. Indeed, the
552 Berman's Z_2 test for the dependence of the point process on the spatial covari-
553 ate x failed to reject the null hypothesis for SU C ($p-value = 0.0044$) and D
554 ($p-value = 1.913e - 14$). However, even if it suggests significant evidence that
555 the intensity depends on some covariate, the effect of that covariate could still
556 be weak. ROC curves (Fig. 5e,f) indicate that the x coordinate does not have
557 discriminatory power.

558 Bartlett (1963) showed that it is possible to formulate a point pattern which
559 can be equally interpreted as a Poisson inhomogeneous process, or a homoge-
560 neous cluster process. According to our non-parametric analyses, we proceeded

under the assumption that the processes involved in the formation of the Pirro Nord (P13) deposit are homogeneous and clustered. The scan tests in Fig. 6a,d show hot spots of points, mostly localized between $6 < x < 7$ and $8 < x < 9$. The cluster correlation between all the finds is significantly confirmed by the estimations of the K and F functions (Fig. 6). The first lines of panels in Fig. 7 and 8 offer a type-based view of these patterns. Indeed, the estimated $\hat{K}(r)$ functions of the faunal assemblage (Fig. 7a and 8a), which constitute the bigger part of the analyzed sample of data, resemble the results for the complete populations (Fig. 6b,e). The lithic assemblage also shows significant aggregation; while the small sample of *A. ruffoi* falls inside the envelope of CSR.

Faunal remains and lithic artifacts show some overlapping when evaluated by means of Gaussian smoothing kernel (Fig. 5c,d). Positive spatial association between fossils and lithics is statistically confirmed by the cross-type K and G functions for the examined SUs (Fig. 7 and 8). Fossils and artifacts tend then to occur aggregated with each other (they are closer than expected for an independent process). Significant spatial proximity is also shown between artifacts and micromammal remains, especially in SU D.

According to the results of our analyses, the stratigraphic and spatial association between the types of remains should be considered as the result of the same formation process. Finds occur in the clayey-sand sediment together with a high number of angular to sub-rounded gravels and boulder-sized rock clasts. Such a stratigraphic setting suggests repeated mass-wasting processes (at least two events, represented by SUs C and D, which were included in this study) with a low degree of reworking in a relatively short span of time (Arzarello et al., 2012). Rapid-moving and chaotic water-laden masses, such as mud-flows or earth-flows, of soilwash and rock rubble with fossils and artifacts (Butzer, 1982, p. 46), could have been triggered by intense rainfalls and became trapped in the karst sink-hole directly opening to the outside. The sedimentary fill would have derived from the top, by gravity, directed into the empty space between the large limestone blocks that made up the internal structure of the fissure. The thickness of the layers is likely correlated to the intensity of such events.

592 On the other hand, the clustered distribution of all the finds cannot be linked
593 to the thickness of the stratigraphic units. The big blocks of calcarenite, which in
594 some places transect the stratigraphic units (Fig. 1), created a complex internal
595 structure and might have influenced the direction of sediment accumulation.
596 However, sedimentation rate, driven by the rugged topography of the site, does
597 not seem to be spatially associated with the localized hot spots (Fig. 6a,d).
598 Thus, clustering might have been a correlated effect of the formation process.

599 The presence of partially articulated vertebrate skeletal elements and their
600 general low degree of weathering indicate fast burial and transport of bones from
601 nearby locations (Bagnus, 2011). A close spatial proximity between the original
602 location of the finds and the karst fissure, as well as a relatively fast burial, is
603 also corroborated by the unrounded ridges and edges of the lithic artifacts and
604 by the technological consistency of the assemblage (Arzarello et al., 2015).

605 In conclusion, our spatial statistics analyses confirm the field observations
606 about the spatial association of archaeological and paleontological remains.

607 *7.2. Post-depositional processes*

608 After dealing with our first research question (to examine the spatial dis-
609 tribution of finds in the context of the site formation processes), our analyses
610 were particularly directed to test the hypothesis of post-depositional processes
611 reworking the deposit. We assume that the spatial aggregation of taphonomic
612 surface alterations, and their relative segregation compared to non-altered finds,
613 would indicate the localized activity of diagenetic agents.

614 We focused more on the spatial distribution of oxides, because traditional
615 explanations for the development of Fe-Mn patinas on the surface of flint refer to
616 the deposition of various iron and manganese oxides and hydroxides out of soil
617 water (Stapert, 1976). Similarly, the origin of manganese coatings on fossils, in
618 karst environments, may derive from circulating water, or from the manganese
619 present in the surrounding limestone rock dissolved by groundwater (Hill, 1982).

620 The vertical distribution of oxides on the lithic artifacts and the sample of
621 faunal remains (Fig. 4) spans the complete stratigraphic sequence and appar-

622 ently shows a gradual increase through the lower layers, especially in the lithic
623 assemblage. Intensity of oxides is indeed more likely proportional to the density
624 of finds and not related to the depth.

625 By applying a set of spatial statistics (namely cross-type $K_{ij}(r)$ function)
626 to the archaeological and paleontological remains, we searched for evidence of
627 localized areas, which might have been subjected to the presence of water, es-
628 pecially water-flows.

629 In SU C, the spatial distribution of Fe-Mn patinas on lithics and fossils
630 is, with a certain degree of significance, the result of independent processes
631 (Fig. 9a,c,d). We cannot state that there is aggregation (spatial proximity)
632 between oxidized finds and fresh ones. Neither the results of the bivariate K
633 function, random labeling the cases/controls of Fe-Mn coating, show segrega-
634 tion, which is indicative of spatially defined diagenetic processes. In contrast, in
635 SU D (Fig. 9b), patinated and fresh artifacts occur significantly spatially aggre-
636 gated to each other for values of $r > 0.4m$. They occur closer than expected by
637 an independent process at bigger scale. However, the pattern is, with a certain
638 confidence level, independent.

639 Rottländer (1975) identified a possible different cause of Fe-Mn coatings in
640 the iron that is already present in the flint. In this light, the spatial association
641 of flint artifacts with and without patination also depends on the chemical and
642 microstructural composition of the raw material itself. On the other hand,
643 the same oxides affecting a good percentage of finds, have been equally found
644 broadly scattered on the numerous clasts of calcarenite that are included in the
645 matrix, thus supporting an external origin of the Fe-Mn coating process.

646 The content of water and organic matter in the sedimentary body could
647 be responsible for the randomly diffuse Fe-Mn patinations. In the presence of
648 organic matter, indeed, it is likely that the release of organic acids will accelerate
649 patination on chert (Burroni et al., 2002). Moisture of the sedimentary body
650 could also be accounted for the wide random spread of Fe-Mn coatings.

651 We did not find statistically significant evidence of aggregation of oxidized
652 records compared to non-oxidized ones (Fig. 9c); thus, we can exclude the as-

653 sumption of localized concentration of water, which is included in the hypothesis
654 advanced by Bagnus (2011) for the presence of interstitial flows reworking the
655 deposit.

656 Due to the small sample size, we did not apply spatial analysis to the distribution
657 of the three taphorecords. However, Fig. 4e,f suggests that fossils from
658 the TR1 group occur spatially aggregated with fossils from the TR2 and TR3
659 groups. Considering the distribution of Fe-Mn oxides on the lithic and faunal
660 assemblages, the re-elaborated TR1 (*sensu* Fernández-López, 1991, 2007, 2011)
661 might not be associated with the reworking action of water-flows and might
662 be more likely correlated to random and limited rearrangement of parts of the
663 sedimentary matrix.

664 A possible cause of some localized movement of sediments could be the rock
665 falls from the vault of the karst fissure, during the deposition of SUs C and D.
666 As showed in Fig. 1, an abrupt increase in the number of boulder-sized rocks is
667 observed within the lower layers. Moreover, rock falls caused most of the post-
668 depositional fractures on the faunal assemblage (Bagnus, 2011). Such intense
669 erosional process could most likely be correlated to the seismic activity of the
670 region (Bertok et al., 2013).

671 Results of our analyses suggest that post-depositional taphonomic alterations
672 occurred with a certain significance as a result of independent processes.
673 However, keeping a cautious approach to spatial analysis, a documented point
674 pattern can be most realistically thought of as the result of multiple processes
675 heterogeneously working at different scales (Bevan and Wilson, 2013). Multiple
676 or repeated post-depositional processes could obliterate contemporaneous or
677 preceding patterns, resulting in a final random distribution of the record.

678 Moreover, karst site formation processes are highly dependent on the structure
679 and extension of the overall karstic system, as well as on the surrounding
680 environment. The lack of information about the original characteristics of the
681 system and the reduced area of excavation strongly limit the analysis.

682 Furthermore, although the need for considering three dimensional distributions
683 in site formation processes study, spatial point pattern statistics are at

684 the moment not fully equipped to analyze three-dimensional patterns, espe-
685 cially when the study-area corresponds to a three-dimensional volume with a
686 complex shape such as a karstic structure.

687 On the other hand, "one must look to non-spatial evidence to corroborate or
688 disprove theories about spatial processes" (Hodder and Orton, 1976, p. 8). The
689 integration with other taphonomic disciplines reinforces the results of spatial
690 analyses and outlines new opportunities for point pattern analyses. As recently
691 remarked (Cobo-Sánchez et al., 2014), taphonomic research should be multi-
692 variate (Domínguez-Rodrigo and Pickering, 2010) and it should include spatial
693 analysis as a heuristic tool in the interpretation of site integrity. This is espe-
694 cially demanding when the research questions deal with past human behaviour
695 and even more so when site dating is based on the stratigraphic association of
696 artifacts and fossils.

697 8. Conclusions

698 The Early Pleistocene site of Pirro Nord 13 provides evidence of the earliest
699 human presence in Western Europe. Lithic artifacts have been found in a karst
700 fissure filling, together with late Villafranchian/early Biharian paleontological
701 remains.

702 The main goals of our study were:

- 703 1. to investigate the depositional processes involved in the formation of the
704 deposit and
- 705 2. to assess the degree of any potential post-depositional reworking of the
706 archaeological and paleontological remains.

707 The integration of spatial point pattern analyses with previous taphonomic
708 studies on the faunal and lithic assemblages allowed us to test different hypothet-
709 ses of site formation and modification processes.

710 On the basis of our analyses,

- 711 1. we consider the deposit to be the result of subsequent events of some
712 type of mass-wasting process, such as a mud-flow or earth-flow, carrying

⁷¹³ rock rubble with fossils and artifacts. The applied set of spatial analyses
⁷¹⁴ confirms, with an adequate level of statistical significance, the assumption,
⁷¹⁵ based on field observations, regarding the spatial association between the
⁷¹⁶ finds.

⁷¹⁷ 2. Based on our taphonomic point pattern analyses of several diagenetic fea-
⁷¹⁸ tures on the lithic and faunal assemblages, we reject the hypothesis of a
⁷¹⁹ substantial post-depositional reworking and mixture of the sedimentary
⁷²⁰ deposit and we corroborate the stratigraphic integrity of the Pirro Nord
⁷²¹ 13 site.

⁷²² Finally, the present study answers the need for a taphonomic perspective
⁷²³ in spatial analysis, by applying well developed quantitative methods in spatial
⁷²⁴ statistics. Point pattern analysis can be very flexible and useful in the investiga-
⁷²⁵ tion of both cultural and taphonomic processes. Until now it has found limited
⁷²⁶ application on taphonomic studies, but, as our study demonstrates, it offers new
⁷²⁷ analytical opportunities to the multidisciplinary study of the complex processes
⁷²⁸ that operate in the formation and modification of archaeological sites. It allows
⁷²⁹ analysts to test multiscalar patterns and to model the taphonomic processes
⁷³⁰ underlying archaeological distributions, which are otherwise difficult to identify
⁷³¹ from the simple visualization of maps, especially for those sites characterized by
⁷³² complex geo-stratigraphic settings.

⁷³³ Acknowledgements

⁷³⁴ DG was supported by the European Research Council Starting Grant No.
⁷³⁵ 283503 (PaGE) awarded to K. Harvati.

⁷³⁶ Fieldworks were financially supported by the University of Ferrara and the
⁷³⁷ Municipality of Apricena. Excavations were possible by permission of the So-
⁷³⁸ printendenza Archeologica della Puglia and Ministero dei Beni e delle Attività
⁷³⁹ Culturali; thanks to the collaboration of Dott.ssa Anna Maria Tunzi; and by
⁷⁴⁰ courtesy of Gaetano and Franco dell'Erba.

⁷⁴¹ We would like to thank all those who attended the excavation campaigns for
⁷⁴² their indispensable cooperation; Julie Arnaud for her * and contribution to the
⁷⁴³ 3D modeling of the site; and Nick Thompson for English proofreading.

⁷⁴⁴ We are grateful to Vangelis Tourloukis and two anonymous reviewers for their
⁷⁴⁵ critical discussions and many constructive comments that helped to improve this
⁷⁴⁶ manuscript.

⁷⁴⁷ **References**

⁷⁴⁸ Anderson, K. L., Burke, A., 2008. Refining the definition of cultural levels at
⁷⁴⁹ Karabi Tamchin: a quantitative approach to vertical intra-site spatial analy-
⁷⁵⁰ sis. *Journal of Archaeological Science* 35 (8), 2274–2285.

⁷⁵¹ Arzarello, M., Marcolini, F., Pavia, G., Pavia, M., Petronio, C., Petrucci, M.,
⁷⁵² Rook, L., Sardella, R., 2007. Evidence of earliest human occurrence in Europe:
⁷⁵³ the site of Pirro Nord (Southern Italy). *Naturwissenschaften* 94, 107–112.

⁷⁵⁴ Arzarello, M., Marcolini, F., Pavia, G., Pavia, M., Petronio, C., Petrucci, M.,
⁷⁵⁵ Rook, L., Sardella, R., 2009. L'industrie lithique du site Pléistocène inférieur
⁷⁵⁶ de Pirro Nord (Apricena, Italie du sud): une occupation humaine entre 1,3
⁷⁵⁷ et 1,7Ma. *L'Anthropologie* 113 (1), 47–58.

⁷⁵⁸ Arzarello, M., Pavia, G., Peretto, C., Petronio, C., Sardella, R., 2012. Evidence
⁷⁵⁹ of an Early Pleistocene hominin presence at Pirro Nord (Apricena, Foglia,
⁷⁶⁰ southern Italy): P13 site. *Quaternary International* 267, 56–61.

⁷⁶¹ Arzarello, M., Peretto, C., 2010. Out of Africa: The first evidence of Italian
⁷⁶² peninsula occupation. *Quaternary International* 223–224, 65–70.

⁷⁶³ Arzarello, M., Peretto, C., Moncel, M.-H., 2015. The Pirro Nord site (Apricena,
⁷⁶⁴ Fg, Southern Italy) in the context of the first European peopling: Conver-
⁷⁶⁵ gences and divergences. *Quaternary International* 389, 255–263.

- ⁷⁶⁶ Baddeley, A., Rubak, E., Turner, R., 2015. Spatial Point Patterns: Methodology
⁷⁶⁷ and Applications with R, in press Edition. Chapman and Hall/CRC Press,
⁷⁶⁸ London.
- ⁷⁶⁹ Bagnus, C., 2011. Analisi tafonomica delle associazione a vertebrati del Pleis-
⁷⁷⁰ tocene Inferiore di Pirro Nord. Ph.D. thesis, Università degli Studi di Torino,
⁷⁷¹ Italy.
- ⁷⁷² Bailey, T., Gatrell, A., 1995. Interactive spatial data analysis. Longman Scien-
⁷⁷³ tific and Technical, Harlow Essex, England.
- ⁷⁷⁴ Bartlett, M. S., 1963. The spectral analysis of point processes. Journal of the
⁷⁷⁵ Royal Statistical Society, Series B 29, 264–296.
- ⁷⁷⁶ Behrensmeyer, A. K., 1978. Taphonomic and ecologic information from bone
⁷⁷⁷ weathering. Paleobiology 4 (2), 150–162.
- ⁷⁷⁸ Behrensmeyer, A. K., 1991. Terrestrial vertebrate accumulations. In: Allison,
⁷⁷⁹ P., Briggs, D. (Eds.), Taphonomy: Releasing the Data Locked in the Fossil
⁷⁸⁰ Record: Topics in Geobiology. Vol. 9. Plenum Press, New York, p. 291–327.
- ⁷⁸¹ Benito-Calvo, A., de la Torre, I., 2011. Analysis of orientation patterns in Oldu-
⁷⁸² vai Bed I assemblages using GIS techniques: Implications for site formation
⁷⁸³ processes. Journal of Human Evolution 61 (1), 50–60.
- ⁷⁸⁴ Bernatchez, J. A., 2010. Taphonomic implications of orientation of plotted finds
⁷⁸⁵ from Pinnacle Point 13B (Mossel Bay, Western Cape Province, South Africa).
⁷⁸⁶ Journal of Human Evolution 59 (3–4), 274–288.
- ⁷⁸⁷ Bertok, C., Masini, F., Donato, V. D., Martire, L., Pavia, M., Zunino, M.,
⁷⁸⁸ Pavia, G., 2013. Stratigraphic framework of the type-locality of Pirro Nord
⁷⁸⁹ mammal Faunal Unit (Late Villafranchian, Apricena, south- eastern Italy).
⁷⁹⁰ Palaeontographica 298 (6), 5–17.
- ⁷⁹¹ Bertran, P., Hetù, B., Texier, J.-P., Steijn, H. V., 1997. Fabric characteristics
⁷⁹² of subaerial slope deposits. Sedimentology 44 (1), 1–16.

- ⁷⁹³ Bertran, P., Lenoble, A., Todisco, D., Desrosiers, P. M., Sørensen, M., 2012.
- ⁷⁹⁴ Particle size distribution of lithic assemblages and taphonomy of Palaeolithic
- ⁷⁹⁵ sites. *Journal of Archaeological Science* 39 (10), 3148–3166.
- ⁷⁹⁶ Bertran, P., Texier, J.-P., 1995. Fabric Analysis: Application to Paleolithic
- ⁷⁹⁷ Sites. *Journal of Archaeological Science* 22 (4), 521–535.
- ⁷⁹⁸ Bertran, P., Émilie Claud, Detrain, L., Lenoble, A., Masson, B., Vallin, L., 2006.
- ⁷⁹⁹ Composition granulométrique des assemblages lithiques, application à l'étude
- ⁸⁰⁰ taphonomique des sites paléolithiques. *Paléo* 18, 7–36.
- ⁸⁰¹ Bevan, A., Conolly, J., 2006. Multiscalar approaches to settlement pattern anal-
- ⁸⁰² ysis. In: Lock, G., Molyneaux, B. (Eds.), *Confronting Scale in Archaeology:*
- ⁸⁰³ *Issues of Theory and Practice*. Springer, New York, pp. 217–234.
- ⁸⁰⁴ Bevan, A., Conolly, J., 2009. Modelling spatial heterogeneity and nonstation-
- ⁸⁰⁵ arity in artifact-rich landscapes. *Journal of Archaeological Science* 36 (4),
- ⁸⁰⁶ 956–964.
- ⁸⁰⁷ Bevan, A., Conolly, J., 2013. *Mediterranean Islands, Fragile Communities and*
- ⁸⁰⁸ *Persistent Landscapes: Antikythera in Long-term Perspective*. Cambridge
- ⁸⁰⁹ University Press, Cambridge.
- ⁸¹⁰ Bevan, A., Crema, E., Li, X., Palmisano, A., 2013. Intensities, interactions,
- ⁸¹¹ and uncertainties: Some new approaches to archaeological distributions. In:
- ⁸¹² Bevan, A., Lake, M. (Eds.), *Computational Approaches to Archaeological*
- ⁸¹³ *Spaces*. Left Coast Press, Walnut Creek, pp. 27–52.
- ⁸¹⁴ Bevan, A., Wilson, A., 2013. Models of settlement hierarchy based on partial
- ⁸¹⁵ evidence. *Journal of Archaeological Science* 40 (5), 2415–2427.
- ⁸¹⁶ Burroni, D., Donahue, R. E., Pollard, A., Mussi, M., 2002. The surface alteration
- ⁸¹⁷ features of flint artefacts as a record of environmental processes. *Journal of*
- ⁸¹⁸ *Archaeological Science* 29 (11), 1277–1287.

- ⁸¹⁹ Butzer, K., 1982. Archaeology as Human Ecology: Method and Theory for a
⁸²⁰ Contextual Approach. Cambridge University Press, New York.
- ⁸²¹ Carbonell, E., Bermudez de Castro, J. M., Pares, J. M., Perez-Gonzalez, A.,
⁸²² Cuenca-Bescos, G., Olle, A., Mosquera, M., Huguet, R., van der Made, J.,
⁸²³ Rosas, A., Sala, R., Vallverdu, J., Garcia, N., Granger, D. E., Martinon-
⁸²⁴ Torres, M., Rodriguez, X. P., Stock, G. M., Verges, J. M., Allue, E., Burjachs,
⁸²⁵ F., Caceres, I., Canals, A., Benito, A., Diez, C., Lozano, M., Mateos, A.,
⁸²⁶ Navazo, M., Rodriguez, J., Rosell, J., Arsuaga, J. L., 2008. The first hominin
⁸²⁷ of Europe. *Nature* 452, 465–469.
- ⁸²⁸ Carrer, F., 2015. Interpreting intra-site spatial patterns in seasonal contexts: an
⁸²⁹ ethnoarchaeological case study from the western alps. *Journal of Archaeolog-*
⁸³⁰ *ical Method and Theory*, 1–25.
- ⁸³¹ Cobo-Sánchez, L., Aramendi, J., Domínguez-Rodrigo, M., 2014. Orientation
⁸³² patterns of wildebeest bones on the lake Masek floodplain (Serengeti, Tan-
⁸³³ zania) and their relevance to interpret anisotropy in the Olduvai lacustrine
⁸³⁴ floodplain. *Quaternary International* 322–323 (0), 277–284.
- ⁸³⁵ Crema, E. R., 2015. Time and probabilistic reasoning in settlement analysis.
⁸³⁶ In: Juan A. Barcelo, I. B. (Ed.), *Mathematics and Archaeology*. CRC Press,
⁸³⁷ Boca Raton, FL, pp. 314–334.
- ⁸³⁸ Crema, E. R., Bevan, A., Lake, M. W., 2010. A probabilistic framework for
⁸³⁹ assessing spatio-temporal point patterns in the archaeological record. *Journal*
⁸⁴⁰ *of Archaeological Science* 37 (5), 1118–1130.
- ⁸⁴¹ Crema, E. R., Bianchi, E., 2013. Looking for patterns in the noise: non-site
⁸⁴² spatial-analysis in Sebkha Kelbia. In: Mulazzani, S. (Ed.), *Le Capsien de*
⁸⁴³ *hergla (Tunisie). Culture, environnement et économie*. Africa Magna Verlag,
⁸⁴⁴ Frankfurt, pp. 385–395.
- ⁸⁴⁵ Crochet, J.-Y., Welcomme, J.-L., Ivorra, J., Ruffet, G., Boulbes, N., Capdevila,
⁸⁴⁶ R., Claude, J., Firmat, C., Métais, G., Michaux, J., Pickford, M., 2009. Une

- ⁸⁴⁷ nouvelle faune de vertébrés continentaux, associée à des artefacts dans le
⁸⁴⁸ Pléistocène inférieur de l'Hérault (Sud de la France), vers 1,57 Ma. Comptes
⁸⁴⁹ Rendus Palevol 8 (8), 725–736.
- ⁸⁵⁰ de la Torre, I., Benito-Calvo, A., 2013. Application of GIS methods to retrieve
⁸⁵¹ orientation patterns from imagery; a case study from Beds I and II, Olduvai
⁸⁵² Gorge (Tanzania). Journal of Archaeological Science 40 (5), 2446–2457.
- ⁸⁵³ Despriée, J., Gageonnet, R., Voinchet, P., Bahain, J.-J., Falguères, C., Varache,
⁸⁵⁴ F., Courcimault, G., Dolo, J.-M., 2006. Une occupation humaine au Pléis-
⁸⁵⁵ tocène inférieur sur la bordure nord du Massif central. Comptes Rendus
⁸⁵⁶ Palevol 5 (6), 821–828.
- ⁸⁵⁷ Despriée, J., Voinchet, P., Gageonnet, R., Dépont, J., Bahain, J.-J., Falguères,
⁸⁵⁸ C., Tissoux, H., Dolo, J.-M., Courcimault, G., 2009. Les vagues de peuple-
⁸⁵⁹ ments humains au Pléistocène inférieur et moyen dans le bassin de la Loire
⁸⁶⁰ moyenne, région Centre, France. Apports de l'étude des formations fluviatiles.
⁸⁶¹ L'Anthropologie 113 (1), 125–167.
- ⁸⁶² Despriée, J., Voinchet, P., Tissoux, H., Moncel, M.-H., Arzarello, M., Robin,
⁸⁶³ S., Bahain, J.-J., Falguères, C., Courcimault, G., Dépont, J., Gageonnet,
⁸⁶⁴ R., Marquer, L., Messager, E., Abdessadok, S., Puaud, S., 2010. Lower and
⁸⁶⁵ middle Pleistocene human settlements in the Middle Loire River Basin, Centre
⁸⁶⁶ Region, France. Quaternary International 223–224, 345–359.
- ⁸⁶⁷ Dibble, H. L., Chase, P. G., McPherron, S. P., Tuffreau, A., Oct. 1997. Testing
⁸⁶⁸ the reality of a "living floor" with archaeological data. American Antiquity
⁸⁶⁹ 62 (4), 629–651.
- ⁸⁷⁰ Diggle, P., 1985. A kernel method for smoothing point process data. Applied
⁸⁷¹ Statistics (Journal of the Royal Statistical Society, Series C) 34, 138–147.
- ⁸⁷² Diggle, P., 2003. Statistical analysis of spatial point patterns. Hodder Arnold,
⁸⁷³ London.

- 874 Djindjian, F., 1999. L'analyse spatiale de l'habitat: un état de l'art. *Archeologia*
875 e Calcolatori X, 17–32.
- 876 Domínguez-Rodrigo, M., Bunn, H., Mabulla, A., Baquedano, E., Uribelarrea,
877 D., Pérez-González, A., Gidna, A., Yravedra, J., Diez-Martín, F., Egeland,
878 C., Barba, R., Arriaza, M., Organista, E., Ansón, M., 2014a. On meat eating
879 and human evolution: A taphonomic analysis of BK4b (Upper Bed II, Oldu-
880 vai Gorge, Tanzania), and its bearing on hominin megafaunal consumption.
881 *Quaternary International* 322–323, 129–152.
- 882 Domínguez-Rodrigo, M., Diez-Martín, F., Yravedra, J., Barba, R., Mabulla, A.,
883 Baquedano, E., Uribelarrea, D., Sánchez, P., Eren, M. I., 2014b. Study of the
884 SHK Main Site faunal assemblage, Olduvai Gorge, Tanzania: Implications
885 for Bed II taphonomy, paleoecology, and hominin utilization of megafauna.
886 *Quaternary International* 322–323, 153–166.
- 887 Domínguez-Rodrigo, M., Fernández-López, S., Alcalá, L., 2011. How Can
888 Taphonomy Be Defined in the XXI Century? *Journal of Taphonomy* 9 (1),
889 1–13.
- 890 Domínguez-Rodrigo, M., Pickering, T., 2010. A multivariate approach for dis-
891 criminating bone accumulations created by spotted hyenas and leopards: har-
892 nessing actualistic data from east and southern Africa. *Journal of Taphonomy*
893 8 (2–3), 155–179.
- 894 Domínguez-Rodrigo, M., Uribelarrea, D., Santonja, M., Bunn, H., García-Pérez,
895 A., Pérez-González, A., Panera, J., Rubio-Jara, S., Mabulla, A., Baquedano,
896 E., Yravedra, J., Diez-Martín, F., 2014c. Autochthonous anisotropy of ar-
897 chaeological materials by the action of water: experimental and archaeolog-
898 ical reassessment of the orientation patterns at the Olduvai sites. *Journal of*
899 *Archaeological Science* 41, 44–68.
- 900 Díez, J. C., Fernández-Jalvo, J., Rossel, J., Cáceres, I., 1999. Zooarchaeology
901 and taphonomy of Aurora Stratum (Gran Dolina, Sierra de Atapuerca, Spain).
902 *Journal of Human Evolution* 37, 623–652.

- 903 Efremov, I. A., 1940. Taphonomy: a new branch of paleontology. Pan American
904 Geologist 74, 81–93.
- 905 Eve, S. J., Crema, E. R., 2014. A House with a View? Multi-model inference,
906 visibility fields, and point process analysis of a Bronze Age settlement on
907 Leskernick Hill (Cornwall, UK). Journal of Archaeological Science 43, 267–
908 277.
- 909 Fernández-López, S. R., 2000. Temas de Tafonomía. Departamento de Paleon-
910 tología, Universidad Complutense de Madrid.
- 911 Fernández-López, S. R., 1987. Unidades registráticas, biocronología y
912 geocrontología. Revista Española de Paleontología 2, 65–85.
- 913 Fernández-López, S. R., 1991. Taphonomic concepts for a theoretical biochronol-
914 ogy. Revista Española de Paleontología 6, 37–49.
- 915 Fernández-López, S. R., 2007. Ammonoid taphonomy, palaeoenvironments and
916 sequence stratigraphy at the Bajocian/Bathonian boundary on the Bas Auran
917 area (Subalpine Basin, SE France). Lethaia 40, 377–391.
- 918 Fernández-López, S. R., 2011. Taphonomic analysis and sequence stratigraphy
919 of the Albarracinites beds (lower Bajocian, Iberian Range, Spain). An exam-
920 ple of shallow condensed section. Bulletin de la Société Géologique de France
921 182, 405–415.
- 922 Gatrell, A. C., Bailey, T. C., Diggle, P. J., Rowlingson, B. S., 1996. Spatial point
923 pattern analysis and its application in geographical epidemiology. Transac-
924 tions of the Institute of British Geographers 21, 256–274.
- 925 Goreaud, F., Pélissier, R., October 2003. Avoiding misinterpretation of biotic
926 interactions with the intertype k_{12} -function: population independence vs. ran-
927 dom labelling hypotheses. Journal of Vegetation Science 14 (5), 681–692.
- 928 Hill, C. A., 1982. Origin of black deposits in caves. National Speleological Society
929 Bulletin 44, 15–19.

- 930 Hodder, I., Orton, C., 1976. Spatial Analysis in Archaeology. New Studies in
931 Archaeology. Cambridge University Press, Cambridge.
- 932 Kos, A. M., 2003. Characterization of post-depositional taphonomic processes
933 in the accumulation of mammals in a pitfall cave deposit from southeastern
934 Australia. Journal of Archaeological Science 30, 781–796.
- 935 Lenoble, A., Bertran, P., 2004. Fabric of Palaeolithic levels: methods and impli-
936 cations for site formation processes. Journal of Archaeological Science 31 (4),
937 457–469.
- 938 Lopez-García, J. M., Luzi, E., Berto, C., Peretto, C., Arzarello, M., 2015.
939 Chronological context of the first hominin occurrence in southern Europe:
940 the *Allophaiomys ruffoi* (Arvicolinae, Rodentia, Mammalia) from Pirro 13
941 (Pirro Nord, Apulia, southwestern Italy). Quaternary Science Reviews 107,
942 260–266.
- 943 Lumley, H., Krzepkowska, A., Echassoux, A., 1988. L'industrie du Pleistocene
944 inférieur de la grotte du Vallonnet, Roquebrune-Cap Martin, Alpes Maritimes.
945 L'Anthropologie 92, 501–614.
- 946 López-González, F., Grandal-d'Anglade, A., Vidal-Romaní, J. R., 2006. Deci-
947 phering bone depositional sequences in caves through the study of manganese
948 coatings. Journal of Archaeological Science 33 (5), 707–717.
- 949 López-Ortega, E., Rodríguez, X. P., Vaquero, M., 2011. Lithic refitting and
950 movement connections: the NW area of level TD10-1 at the Gran Dolina
951 site (Sierra de Atapuerca, Burgos, Spain). Journal of Archaeological Science
952 38 (11), 3112–3121.
- 953 McPherron, S. J., 2005. Artifact orientations and site formation processes from
954 total station proveniences. Journal of Archaeological Science 32 (7), 1003–
955 1014.

- 956 Ohser, J., 1983. On estimators for the reduced second moment measure of point
957 processes. *Mathematische Operationsforschung und Statistik, series Statistics*
958 14, 63–71.
- 959 Openshaw, S., 1996. Developing GIS-relevant zone-based spatial analysis meth-
960 ods. In: Longley, P., Batty, M. (Eds.), *Spatial analysis: modelling in a GIS*
961 environment. *Geoinformation International*, London, pp. 55–73.
- 962 Ord, J. K., 1972. Density estimation and tests for randomness, using distance
963 methods. Draft for lecture to Advanced Institute on statistical ecology in the
964 United States, The Pennsylvania State University, (Mimeo).
- 965 Orton, C., 1982. Stochastic process and archaeological mechanism in spatial
966 analysis. *Journal of Archaeological Science* 9 (1), 1–23.
- 967 Orton, C., 2004. Point pattern analysis revisited. *Archeologia e Calcolatori* 15,
968 299–315.
- 969 Parés, J. M., Pérez-González, A., Rosas, A., Benito, A., de Castro, J. B., Car-
970 bonell, E., Huguet, R., 2006. Matuyama-age lithic tools from the Sima del
971 Elefante site, Atapuerca (northern Spain). *Journal of Human Evolution* 50 (2),
972 163–169.
- 973 Petraglia, M. D., Nash, D. T., 1987. The impact of fluvial processes on experi-
974 mental sites. In: Nash, D. T., Petraglia, M. D. (Eds.), *Natural formation pro-*
975 *cesses and the archaeological record*. Vol. 352 of *International Series. British*
976 *Archaeological Reports*, Oxford, pp. 108–130.
- 977 Petraglia, M. D., Potts, R., 1994. Water Flow and the Formation of Early Pleis-
978 tocene Artifact Sites in Olduvai Gorge, Tanzania. *Journal of Anthropological*
979 *Archaeology* 13 (3), 228–254.
- 980 R Core Team, 2015. R: A Language and Environment for Statistical Computing.
981 R Foundation for Statistical Computing, Vienna, Austria.

- 982 Ripley, B., 1988. Statistical inference for spatial processes. Cambridge University
983 Press.
- 984 Ripley, B. D., 1976. The second-order analysis of stationary point processes.
985 Journal of Applied Probability 13 (2), 255–266.
- 986 Ripley, B. D., 1977. Modelling spatial patterns. Journal of the Royal Statistical
987 Society, series B 39, 172–212.
- 988 Robert, C., Casella, G., 2004. Monte Carlo Statistical Methods, second edition
989 Edition. Springer Texts in Statistics. Springer New York, New York.
- 990 Rottländer, R., 1975. The formation of patina on flint. Archaeometry 17 (1),
991 106–110.
- 992 Schick, K. D., 1984. Processes of Paleolithic site formation: an experimental
993 study. Ph.D. thesis, University of California, Berkeley, US.
- 994 Schick, K. D., 1986. Stone Age sites in the making: experiments in the formation
995 and transformation of archaeological occurrences. Vol. 319 of International
996 Series. British Archaeological Reports, Oxford.
- 997 Schiffer, M. B., 1972. Archaeological Context and Systemic Context. American
998 Antiquity 37 (2), 156–165.
- 999 Schiffer, M. B., 1983. Toward the identification of formation processes. American
1000 Antiquity 48 (4), 675–706.
- 1001 Schiffer, M. B., 1987. Formation processes of the archaeological record. University
1002 of New Mexico Press, Albuquerque.
- 1003 Sisk, M. L., Shea, J. J., 2008. Intrasite spatial variation of the Omo Kibish
1004 Middle Stone Age assemblages: Artifact refitting and distribution patterns.
1005 Journal of Human Evolution 55 (3), 486–500.
- 1006 Stapert, D., 1976. Some natural surface modifications on chert in the Nether-
1007 lands. Palaeohistoria 18, 7–41.

- 1008 Texier, J.-P., 2000. A propos des processus de formation des sites préhistoriques
1009 / About prehistoric site formation processes. *Paléo* 12 (1), 379–386.
- 1010 Tobler, W. R., 1970. A computer movie simulating urban growth in the Detroit
1011 region. *Economic Geography* 46 (2), 234–240.
- 1012 Toro-Moyano, I., Barsky, D., Cauche, D., Celiberti, V., Grégoire, S., Lebegue,
1013 F., Moncel, M. H., de Lumley, H., 2011. The archaic stone tool industry from
1014 Barranco León and Fuente Nueva 3, (Orce, Spain): Evidence of the earliest
1015 hominin presence in southern Europe. *Quaternary International* 243 (1), 80–
1016 91.
- 1017 Toro-Moyano, I., de Lumley, H., Fajardo, B., Barsky, D., Cauche, D., Celiberti,
1018 V., Grégoire, S., Martínez-Navarro, B., Espigares, M. P., Ros-Montoya, S.,
1019 2009. L'industrie lithique des gisements du Pléistocène inférieur de Barranco
1020 León et Fuente Nueva 3 à Orce, Grenade, Espagne. *L'Anthropologie* 113 (1),
1021 111–124.
- 1022 Toro-Moyano, I., Martínez-Navarro, B., Agustí, J., Souday, C., de Castro, J. B.,
1023 Martinón-Torres, M., Fajardo, B., Duval, M., Falguères, C., Oms, O., Parés,
1024 J., Anadón, P., Julià, R., García-Aguilar, J., Moigne, A.-M., Espigares, M.,
1025 Ros-Montoya, S., Palmqvist, P., 2013. The oldest human fossil in Europe,
1026 from Orce (Spain). *Journal of Human Evolution* 65 (1), 1–9.
- 1027 Torres, T., Ortiz, J. E., Cobo, R., 2003. Features of deep cave sediments: their
1028 influence on fossil preservation. *Estudios Geológico* 59, 195–204.
- 1029 Villa, P., 1982. Conjoinable Pieces and Site Formation Processes. *American
1030 Antiquity* 47 (2), 276–290.
- 1031 Whallon, R. J., 1974. Spatial analysis of occupation floors ii: The application
1032 of nearest neighbor analysis. *American Antiquity* 39 (1), 16–34.
- 1033 White, W. B., 1976. Cave minerals and speleothems. In: Ford, T., Cullingford,
1034 C. (Eds.), *The Science of Speleology*. Academic Press, London, pp. 267–327.

- ¹⁰³⁵ White, W. B., Vito, C., Scheetz, B. E., 2009. The mineralogy and trace element
¹⁰³⁶ chemistry of black manganese oxide deposits from caves. *Journal of Cave and*
¹⁰³⁷ *Karst Studies* 71 (2), 136–143.
- ¹⁰³⁸ Wood, R. W., Johnson, D. L., 1978. A survey of disturbance processes in archaeo-
¹⁰³⁹ logical site formation. In: Schiffer, M. B. (Ed.), *Advances in archaeological*
¹⁰⁴⁰ *method and theory*. Vol. 1. Academic Press, New York, Ch. 9, pp. 315–381.